Available at www.sciencedirect.com

ScienceDirect

journal homepage: www.elsevier.com/locate/issn/15375110

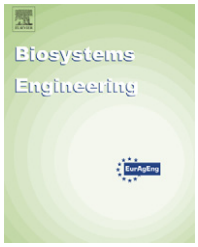

Research Paper

Development of carbon dioxide (CO_2) sensor for grain quality monitoring

S. Neethirajan [a], M.S. Freund [b,c,*], D.S. Jayas [a,*], C. Shafai [c], D.J. Thomson [c], N.D.G. White [d]

[a] Department of Biosystems Engineering, University of Manitoba, Winnipeg, MB, Canada R3T 5V6
[b] Department of Chemistry, University of Manitoba, Winnipeg, MB, Canada R3T 2N2
[c] Department of Electrical and Computer Engineering, University of Manitoba Winnipeg, MB, Canada R3T 5V6
[d] Agriculture and Agri-Food Canada, Cereal Research Centre, Winnipeg, MB, Canada R3T 2M9

ARTICLE INFO

Article history:
Received 9 December 2009
Received in revised form
24 April 2010
Accepted 4 May 2010
Published online 9 June 2010

A carbon dioxide sensor was developed using polyaniline boronic acid conducting polymer as the electrically conductive region of the sensor and was demonstrated for use in detecting incipient or ongoing spoilage in stored grain. The developed sensor measured gaseous CO_2 levels in the range of 380–2400 ppm of CO_2 concentration levels. The sensor was evaluated for the influence of temperature (at - 25 °C to simulate storage and for the operating temperature range of +10 °C to +55 °C) as well as relative humidity (from 20 to 70%). The variation in the resistance with humidity was curvilinear and repeatable, and had a less pronounced effect on the sensor's performance compared to temperature. The sensor was able to respond to changes in CO_2 concentration at various humidity and temperature levels. The response of the PABA film to CO_2 concentration was not affected by the presence of alcohols and ketones at 1% of vapour pressure, proving that the developed sensor is not cross-sensitive to these compounds which may be present in spoiling grain. The sensor packaging components were selected and built in such a way as to avoid contamination of the sensing material and the substrate by undesirable components including grain dust and chaff. The developed conducting polymer carbon dioxide sensor exhibited effective response, recovery time, sensitivity, selectivity, stability and response slope when exposed to various carbon dioxide levels inside simulated grain bulk conditions.

1. Introduction

The world annual grain production is about 2 Gt (billion metric tonnes) (USDA, 2007). Stored grain bulks are ecological systems where communities of insects, mites and microflora interact with abiotic variables to cause spoilage (Wallace & Sinha, 1981). While the importance of proper grain storage has been realised, post-harvest losses continue to range from 9% in North America to 50% in developing countries (FAO, 2000). Any loss in quality or quantity of the produced grain has far-reaching economic effects.

During the spoilage of grain, CO_2, moisture and heat are produced by the metabolism of the grain, fungi, insects and mites, and distinct odours are released. Increased levels of CO_2 in a stored grain bulk indicate that insects, mould, or excessive respiration are present. Evolution of excessive CO_2 from a stored grain mass is a reliable indicator of deteriorating grain. Carbon dioxide is also used as a fumigant for insect

* Corresponding authors.
E-mail addresses: michael_freund@umanitoba.ca (M.S. Freund), digvir_jayas@umanitoba.ca (D.S. Jayas).
1537-5110/$ – see front matter © 2010 IAgrE. Published by Elsevier Ltd. All rights reserved.
doi:10.1016/j.biosystemseng.2010.05.002

control during grain storage. During fumigation, there is a need to measure the CO_2 concentration throughout the grain mass to ensure uniform distribution and maintenance of CO_2 concentration. Intergranular air temperature and air composition will help to identify the location of spoilage inside the grain bulk.

Instruments capable of sensing CO_2 concentrations of 0.1% (atmospheric levels are 0.038%) will detect spoilage during stored grain in 80% of deteriorating bulks in farm granaries (Muir, Waterer, & Sinha, 1985). Simulation models of Singh (Jayas), Muir, and Sinha (1983) and experimental data of Muir et al. (1985) concluded that in the absence of prior knowledge of the location of potential deterioration of grain, a sensor capable of detecting CO_2 levels of 2 g m^{-3} should be located near the centre of the bin. Ileleji, Maier, Bhat, and Woloshuk (2006) employed commercial CO_2 sensors near the vents and exhaust air stream of fans in the grain bin for measuring CO_2. They concluded that hot spot and early spoilage of grain can be detected inside grain bins using CO_2 sensors. Measurement of the intergranular CO_2 inside grain bulk remains a challenging task, mainly because of lack of availability of sensors and deployment issues.

The correlation between different ppm levels of CO_2 and indication of infestation in grain stores has been established by Semple, Hicks, Lozare, and Castermans (1988) (Table 1). A detailed overview of the types of CO_2 sensors, their sensing mechanisms and characteristics covering different aspects of the CO_2 sensor technology has been synthesised by Neethirajan, Jayas, and Sadistap (2009). Most commercially available microfabricated sensors (e.g., Cole–Palmer, Chicago, USA; Figaro Engineering Inc., Osaka, Japan) are made of a substrate heated by wire and coated with a metal oxide, semiconducting film. These sensors rely on the changes of conductivity induced by the adsorption of gases and subsequent surface reactions. These micromachined sensors operate at a relatively high temperature of 200–450 °C which results in significant power consumption. The sensors cannot function without small heaters (usually platinum or gold) on the back side to keep the sensors at operating temperatures. Because of the high operating temperatures, metal oxide sensors are inappropriate in potentially flammable (Dickinson, White, Kauer, & Walt, 1998) or explosive environments such as grain stores. Metal oxide based gas sensors are not recommended to monitor quality of food because irreversible binding of sulphur compounds may cause poisoning (Schaller, Bosset, & Escher, 1998).

Table 1 – Carbon dioxide concentrations as an index of infestation in grain stores. Source: Semple et al. (1988).

CO_2 Concentration (ppm)	Indication of infestation
380 to 500	Atmospheric concentration (no spoilage)
<1100	Incipient spoilage
1100 to 3500	Slight insect infestation and (or) infestation of microorganisms
3500 to 5000	High insect infestation and (or) a higher infection of microorganisms
5000 to 9000	Severe spoilage and limit of dangerous storage conditions
>10,000	Highly unsuitable storage conditions

With the advent of novel polymer materials and micro-nanotechnology, CO_2 micro-sensors can be fabricated and deployed inside grain bulks to measure the intergranular air composition. Polymer films are multifunctional, useful, economical, and practical in a wide range of applications and sensor designs. Miniaturisation of microelectronics favours the use of polymer thin films in sensors. The polyaniline boronic acid (PABA) has been used as a promising sensing material for developing a saccharide sensor (Shoji & Freund, 2002); a conductometric sensor for dopamine detection (Fabre & Taillebois, 2003); and an amine vapour detection sensor (English, Deore, & Freund, 2006). The electrochemical potential of the polymer PABA is sensitive to changes in the pKa (acid dissociation constant) of the polymer as a result of its interaction with change in analyte concentrations (Shoji & Freund, 2002). The pH-dependent equilibria of PABA and its similarity in sensitivity to pH changes to that of polyaniline has been studied by Deore, Braun, and Freund (2006) and Deore & Freund (2009). The added advantages of using PABA as a sensing material for CO_2 detection are: the ability to be used as a simple physical dispersion process for electrode deposition, high environmental stability, and its water solubility during electrochemical polymerisation.

The objectives of this study were to:

1) develop and characterise a prototype CO_2 sensor using PABA, nafion electrolyte and selective gas permeable membranes;
2) evaluate the developed sensor for the effects of temperatures, relative humidity, and presence of selected chemical compounds; and
3) test prototype sensor for measuring varying gaseous CO_2 concentrations in simulated grain bulks.

2. Materials and methods

2.1. *Gas flow management system*

An efficient gas flow management system is crucial for successful sensor characterisation. The gas flow management and the sensor evaluation system consist of a flow system to control the desired gas flow rates to the Teflon testing chamber, and a data collection system to record data from the sensor. Based on our design and input, an automated vapour delivery system was custom built by Plasmionique Inc., St Hyacinthe, PQ to control the flow rate of carbon dioxide and nitrogen gas using mass flow controllers and solenoid valves for delivering the known concentration of CO_2 to a Teflon gas mixing chamber and then to the sensor-testing chamber. This system allowed mixtures of analyte to be produced at various flow rates and at desired concentrations of analyte solutions. Commercially available gas cylinders (Praxair, Edmonton, AB) with a blend of CO_2/air mixture of 9820 ppm concentration and a nitrogen cylinder of ultra high purity (99.99%) were used for the measurements. To achieve the required ppm levels of CO_2 concentrations, gas from 9820 ppm level was diluted to

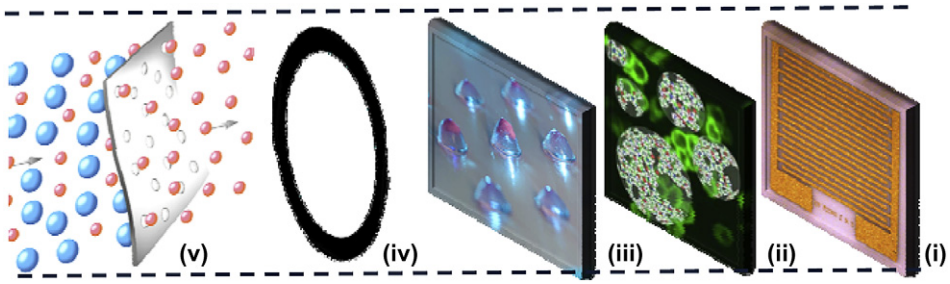

Fig. 1 – Pictorial cross-sectional view of the CO_2 sensor (i) Gold interdigitated electrode PCB array, (ii) PABA polymer, (iii) Nafion, (iv) O-ring, (v) Gas permeable membrane.

appropriate concentrations by mixing and varying the gas flow rate from the nitrogen cylinder.

2.2. Data collection system

The data collection system used for characterisation of the CO_2 sensor consists of an Agilent 34980A Data Acquisition Switch Unit (Agilent Technologies, Inc., Santa Clara, CA). The dc resistance of the sensor was read sequentially by the Agilent data acquisition unit. The control computer was interfaced with the data collection system through an IEEE general purpose interface board (GPIB). The resistance data were initially stored in the data acquisition unit and once a complete set of data was recorded, the GPIB communications software sent the data to the control computer where the data were stored in a tab-limited text file. The gas flow management system and the data collection system were interlinked and connected through a LabVIEW (National Instruments Corporation, Austin, TX) algorithm to control and simultaneously record the gas mixture readings and the sensor response output values.

2.3. Materials

The reagents, chemicals and adhesives including 3-aminophenylboronic acid, polyaniline, phosphoric acid, sodium fluoride, ammonium persulfate, polyvinyl alcohol, potassium chloride, nafion, cyanoacrylate (Permabond 105), polyvinyl chloride, used for the sensor construction were of analytical grade and purchased from Sigma–Aldrich Inc (St. Louis, MO). All aqueous and buffer solutions were prepared with 18.2 MΩ quality deionised water using an ultrapure water system (Millipore Corporation, Billerica, MA). Carbon dioxide porous PTFE membranes 60 μm thick and with average pore diameter of 0.2 μm were acquired from Thermo Scientific (Waltham, MA). Chemically resistant perfluoroelastomer O-rings of 0.3 mm diameter and 0.1 mm wall thickness used for mounting the PTFE gas permeable membrane were purchased from Fisher Scientific (Pittsburgh, PA).

2.4. PABA film synthesis

Poly(anilineboronic acid)/phosphate nanoparticle dispersions were produced using the reactivity of the boronic acid moiety with phosphate in the presence of fluoride (Deore and Freund, 2009). The PABA dispersion solution was synthesised chemically using 10 mM 3-APBA (monomer 3-aminophenylboronic acid) + 50 mM NaF + 5 mM ammonium persulphate (oxidant) in 0.1 M phosphoric acid. The chemical synthesis of PABA polymer is easily water dispersible, and hence it facilitated the formation of smooth, adherent and uniform thin films on the electrode surface. The PABA nanoparticles were in the range of 25–50 nm diameter. The dispersed PABA nanostructures prepared in 0.1 M phosphoric acid with a concentration of 5 mg ml^{-1} was used as the sensing material of the sensor.

2.5. Sensor construction

A cross-sectional and a schematic side view of the constructed sensor assembly are shown in Figs. 1 and 2, respectively. Gold interdigitated array electrodes (IDAs), to be used as the sensor substrate platform, were deposited on a 1 mm thick printed circuit board (PCB), custom designed upon consultation with Iders Inc, Winnipeg, MB. The sensor chip was fabricated by Dynamic & Proto Circuits Inc, Stoney Creek, ON. Each sensor chip has seven sensor elements (detectors) (Fig. 3). The dimensional details of the interdigitated electrode are shown in Fig. 4. A 2 μl drop of PABA solution was deposited on the IDAs through a micropipette as a physical dispersion process and was allowed to dry for 20 min. A 2 μl drop of Nafion

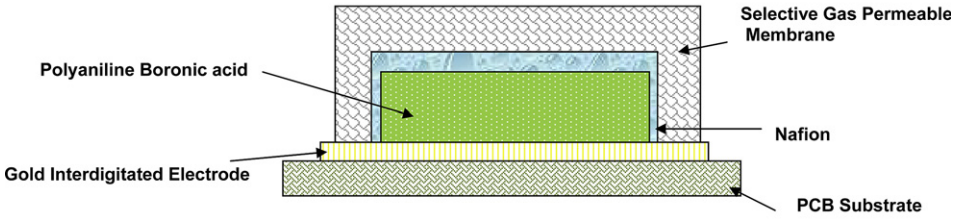

Fig. 2 – Schematic side view of the constructed CO_2 sensor.

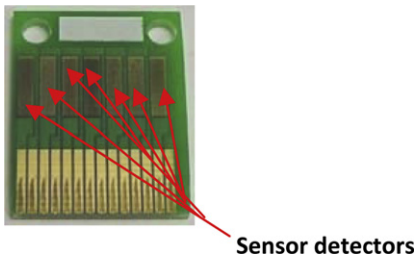

Fig. 3 – Custom built sensor chip showing 7 detectors.

solution was superimposed directly on top of the PABA thin film in the electrically conductive region of the sensor. The solution was then allowed to evaporate in air at 25 °C, and a dried residue was left to form the conductive sensing material. The polytetrafluoroethylene (PTFE) CO_2 selective gas permeable membrane (Sterlitetech Corporation, WA) was applied directly on top of the dried residue of the Nafion electrolyte with the aid of an O-ring. The membrane was cut into circular shapes of approximately 11 mm diameter and was attached to the O-rings by applying small amounts of cyanoacrylate adhesive. The O-ring with the mounted membranes was glued carefully to the PCB substrate of the sensor assembly, forming a cavity with the electrolyte/hydrogel composite and the PABA thin film below the membrane. Care was taken to apply the adhesive only on the rim of the O-ring and thereby avoiding the adhesive contact with the sensing material. The gap between the gas permeable membrane and the surface of the electrolyte/hydrogel composite was kept at a minimum distance (<0.2 mm) using an O-ring to maintain the thin layers of the electrolyte and sensing material.

3. Results and discussion

3.1. Sensor principle

The sensing mechanism is based on the interconversion between conducting emeraldine salt form and the insulating emeraldine base form of polyaniline and PABA through protonation and deprotonation.

When the analyte (gaseous CO_2) permeates through the gas permeable membrane, CO_2 reacts with water from the nafion electrolyte to create a bicarbonate ion (HCO_3–) and a proton, which protonates the polyaniline. When the CO_2 diffuses through the gas-permeable membrane, the following equilibria are sequentially established (Jensen & Rechnitz, 1979).

$$CO_2(aq) + H_2O \rightleftarrows H_2CO_3 \quad (1)$$

$$H_2CO_3 \rightleftarrows H^+ + HCO_3^- \quad (2)$$

$$HCO_3^- \rightleftarrows H^+ + CO_3^{2-} \quad (3)$$

As the CO_2 partial pressure increases, the conductivity increases due to increase in the amount of protonation. This changes the pH of the internal electrolyte. The potential changes linearly with the pH and thereby the concentration of the analyte can be measured. The potential of the electrode depends on the activities of hydronium ions. The Nernst equation (Eq. (4)) relates the potential of electrochemical cell (or sensing assembly) as a function of concentration of ions in the reaction.

$$E = E_0 - \frac{RT}{nf}\ln(Q) \quad (4)$$

where Q is reaction coefficient and n is the number of electrons exchanged. The Nernst equation accurately predicts cell potentials when the equilibrium quotient Q is expressed in ionic activities. The sensors were placed in the Teflon test chamber and were exposed, alternately, to clean dry background air and air containing analyte. The sensor exposures alternated between 5 min of clean background air and 5 min of different analyte concentrations for each analyte concentration. Baseline resistance for each sensor was established by flowing background air (air containing 380 ppm of CO_2) at 0% humidity prior to various nitrogen and CO_2 exposure levels. Sensor data were recorded as resistance versus time and the events such as an exposure to various CO_2 levels or a change in humidity or temperature were analysed as normalised changes in resistance ($\Delta R_m/R_b$).

$$\frac{\Delta R_m}{R_m} = \frac{(R_m - R_b)}{R_b} \quad (5)$$

R_m = sensor resistance at the plateau of the response
R_b = resistance prior to the event

The data was processed using background determination as R_b prior to an exposure of analyte to correct for baseline drift (Jurs, Bakker, & McClelland, 2000).

3.2. Effect of humidity

For functional feasibility, the sensor industry prefers solid electrolyte over liquid electrolyte to maintain compactness of sensor cells considering the size of packaging components, leakage, and drying up of liquid electrolyte under low

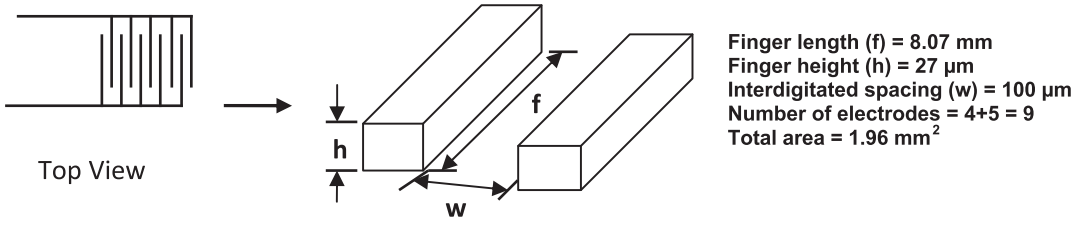

Fig. 4 – Schematic of interdigitated gold electrodes.

humidity/high temperature conditions. Among the solid electrolyte polymers known, Nafion is the best in terms of conductivity and chemical resistance properties (Hu, Vincenzo, Vincenzo, Antonino, & Vincenzo, 2008; Viswanathan & Helen, 2007). Nafion functions as an acid catalyst due to strongly acidic properties of the sulfonic acid group, and also as an ion exchange resin. Interconnections between the sulfonic acid groups in the nafion thin film helps in the rapid transfer and absorption of water and thereby support the sensing material. Nafion has been widely used as a proton exchange membrane in polymer electrode fuel cell applications. The sensor chips prepared with only PABA and without Nafion did not respond to different concentrations of CO_2 below 40% RH (data not shown). For protonation to occur to facilitate the exchange of ions upon exposing to analyte, PABA requires water molecules. The results of the relationship between resistance and CO_2 concentration for the PABA–Nafion sensor under various humidity (RH) levels are shown in Fig. 5. It has been reported (Skotheim, Elsenbaumer, & Reynolds, 1998) that the conductivity of conducting polymers increases when the film absorbs the moisture. The resistance value of PABA decreased with humidity level due to the possibility of proton exchange between the water molecules and the protonated and the unprotonated forms of PABA.

PABA–Nafion sensor showed a two step sensing response to humidity levels. The resistance value of the sensor electrodes decreased when RH increased from 20 to 50% indicating that the water molecules had been absorbed by the PABA film. The charge transfer process of conducting species with water molecules resulted into the decrease in the resistance value. The resistance values of the sensor increased when RH increased from 50% to 70%. The mechanism of charge transfer process may be different for the humidity levels between 50 and 70% RH. The deviation in the linearity could be attributed to the size of the pores of polymer. Similar deviation in the linearity behaviour was observed by Parvatikar, Jain, Khasim et al. (2006) in a Polyaniline (PANI)/tungsten oxide composite sensor when exposed to humidity levels between 20 and 90% RH. In the characterisation of PANI/tungsten composite, the resistance is found to drop down from 20 to 50% RH in a linear fashion while, after 60% RH, saturation is observed with a very small decrease in the resistance up to 90% RH. They speculated that between 20 and 50% RH level, the hole concentration is increased by donation of the lone pair from the conducting complex towards the tungsten oxide water molecules. Thus, the partial charge transfer process of conducting species with that of water molecules resulted in the decreased sheet resistivity. For higher humidity levels above 50% RH, the mechanism may be different leading to the two-step response of the sensor.

Characterisation of polypyrrole-iron oxide composites (Suri, Annapoorni, Sarkar, & Tandon, 2002) as a sensing material for CO_2 sensor with SEM and TEM showed that the presence of fibrillar morphology with macroscopic voids in the material influenced the sensitivity as it facilitated higher permeability to gases. The permeability of gases into the sensing material also depends on the size of the pores and on the kinetic diameter of the gas molecule (Breck, 1974). The role of pore size in humidity sensing by Ag–polyaniline nanocomposite (Fuke et al., 2008), polyaniline/cobalt oxide composites (Parvatikar, Jain, Kanamadi et al., 2006), and polyaniline solid fibres (Ostwal et al., 2005) determined by material characterisation using SEM, XRD, UV, FTIR and spectroscopic techniques showed that the porosity and the pore size influenced the sensitivity of the sensing material.

As the humidity increases from 20% to 50% RH, there may be more hydrogen carbonate ions and protons produced on the PABA film, thus lowering the resistance of the film. The polymer might swell due to water absorption and there may be breakdown or increase in contact between the dispersed conductive nanoparticles affecting the resistance value with the change in humidity. Above 50% RH level, the pores might be saturated with water molecules causing a change in diffusion pathways. The variation in the resistance parameter was curvilinear and repeatable. The film's response to change in analyte concentrations at various humidity levels was very stable until 70% RH and becomes noisy above 70% RH. At humidity levels above 70% RH, the sensors might still perform well when provided with rugged membrane protection and a proper sensor packaging. Irrespective of the change in resistance values at different humidity levels, all the PABA–Nafion sensors responded to various levels of CO_2 concentrations up to 2455 ppm.

The variation in the resistivity as a function of relative humidity value for the PABA sensor is depicted in the Fig. 6.

The percentage sensitivity as a response to humidity is defined as:

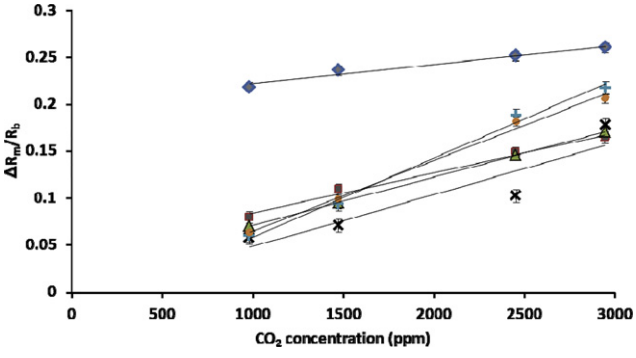

Fig. 5 – Variation of resistance with change in relative humidity (%) for PABA–Nafion sensor at 25 °C. ◆ 20% RH ■ 30% RH ▲ 40% RH X 50% RH + 60% RH ● 70% RH.

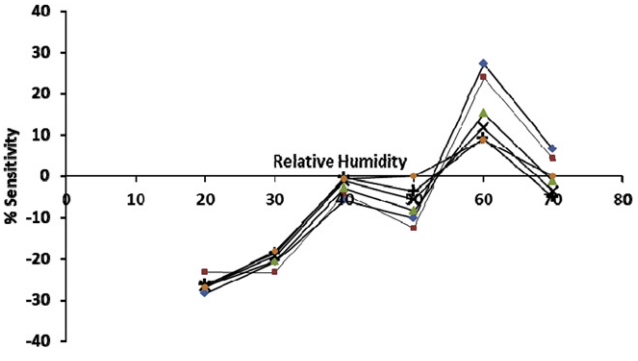

Fig. 6 – Variation of sensitivity to varying CO_2 concentrations with change in relative humidity (%) for PABA–Nafion sensor at 25 °C. ◆ 982 ppm ■ 1473 ppm ▲ 2455 ppm X 2946 ppm + 3682 ppm ● 4910 ppm.

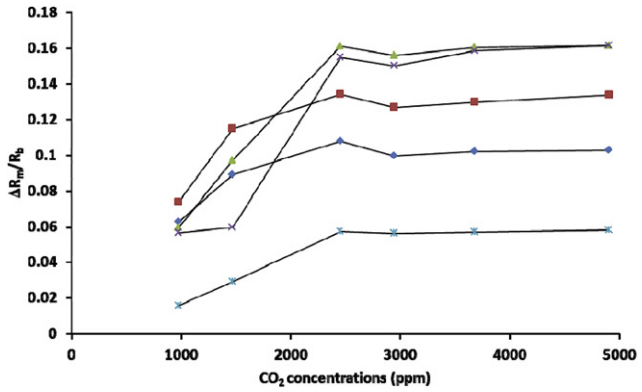

Fig. 7 – Response of PABA–Nafion sensor to varying CO_2 concentrations at 50% RH level and at changing temperature (°C) levels. ♦ – 25 °C ■ +25 °C ▲ +35 °C X + 45 °C ✳ + 55 °C.

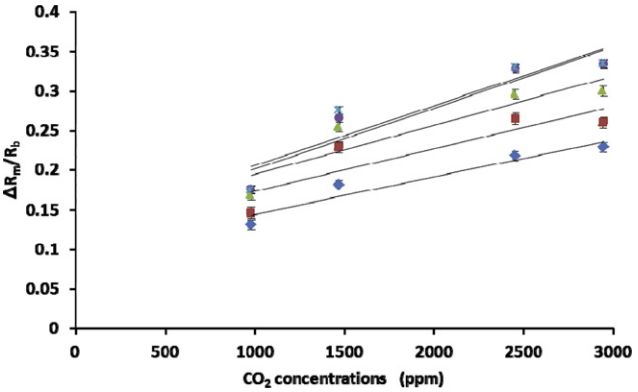

Fig. 9 – Response of PABA–Nafion Sensor Chip #64 (same electrode) to various concentrations of CO_2 at 40% RH and at 25 °C. ♦ Trail 1 ■ Trial 2 ▲ Trial 3 X Trial 4 ● Trial 5.

$$S = \left[\frac{(RH2 - RH1)}{RH1}\right] \times 100 \quad (6)$$

where RH2 is the resistivity of the PABA sensor for humidity at level 2, and RH1 the resistivity of the PABA sensor for humidity at level 1.

The sensor electrodes display a saturation effect above 2455 ppm of CO_2. The sensor's working principle depends on the extraction of ions due to the change in protonation state from the PABA film. Changing the morphology of films by creating a higher surface area through nanorods or nanofibre structures in the polyaniline film might enhance the sensitivity and response time of the sensor (Virji, Huang, Kaner, & Weiller, 2004). Further research is required to explore the possibility of enhancing the response time and sensitivity of PABA thin film by varying morphology. The larger the porous structure of the PABA thin film, the larger will be the reaction surface and inner space for the electrolyte penetration into the film. So, this might shorten the diffusion pathways for the counter ions leading to a quicker response time.

3.3. *Effect of temperature*

The influence of temperature on the performance of the constructed sensors was evaluated by allowing the analyte gas to pass through a copper coil immersed in a heated water bath circulator (Model 12108-20 Cole–Parmer Instrument Company, Vernon Hills, IL). The temperature range was maintained from 25 °C to 55 °C. The sensor chip was also tested at various CO_2 levels after storing the chip at –25 °C for 48 h and then at room temperature for about 2 h before placing it in the testing chamber at 25 °C. The temperature of the analyte gas inside the testing chamber was monitored using a temperature sensor (Model 44 034 Ω Precision Thermistor, Omega Engineering Inc, Stamford, CT).

For the PABA–Nafion sensor, the resistance value decreased from 6000 to 1044 Ω when the temperature increased from 25 °C to 55 °C when exposed to 2400 ppm CO_2. Experiments were conducted by changing the order of heating the CO_2 gas flow and similar trend was observed indicating that the phenomenon is reversible irrespective of the temperature order. The decrease in the resistance value upon increase in temperature (Fig. 7) may be due to the loss of protonation and expulsion of water molecules from the polymer composite. In terms of thermal stability, the influence of the acid used for the protonation of PANI is more than the polyaniline backbone itself, because polyaniline has the ability to sustain exposure to an elevated temperature of 173 °C without damage (Prokes & Stejskal, 2004). Thermogravimetric analysis of PABA by Yu et al. (2005) demonstrated

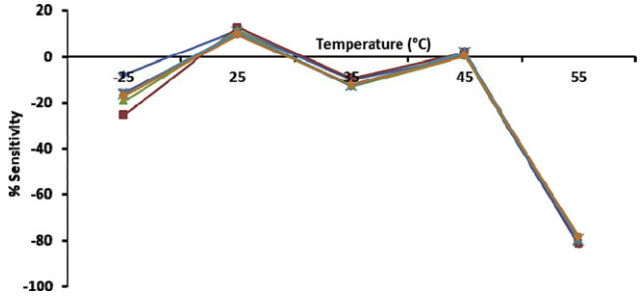

Fig. 8 – Variation of sensitivity with change in temperature (°C) for PABA–Nafion sensor at 50% RH level (Note break in temperature scale below 25 °C). ♦ 982 ppm ■ 1473 ppm ▲ 2455 ppm X 2946 ppm + 3682 ppm ● 4910 ppm.

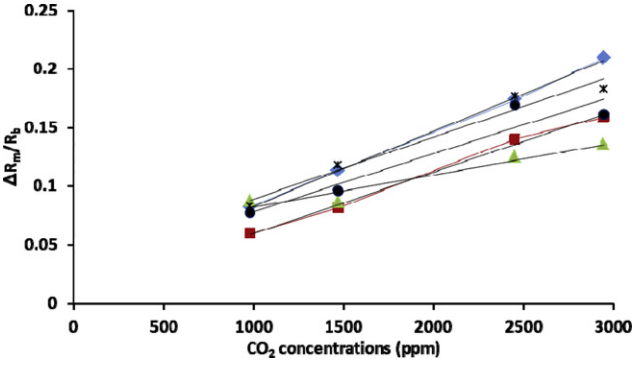

Fig. 10 – Response of 5 different similarly constructed PABA–Nafion sensors to various concentrations of CO_2 at 40% RH and at 25 °C. ♦ Chip #273 ■ Chip #65 ▲ Chip #237 ● Chip #270 X Chip #249.

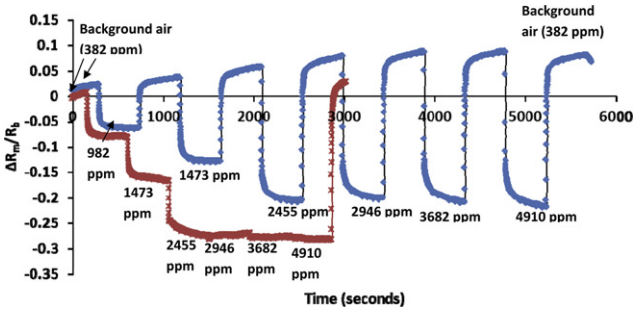

Fig. 11 – Response of the PABA–Nafion sensor operated in step and ramp mode to various concentrations of CO_2 and subsequent exposure to background air at 40% RH and at 25 °C. ◆ Step Mode X Ramp Mode.

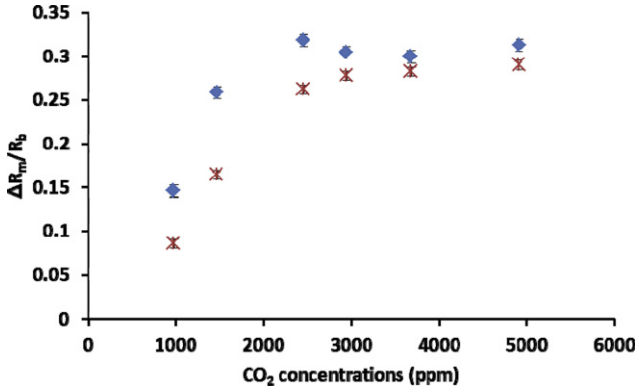

Fig. 13 – Response of the PABA sensor with and without selective gas permeable PTFE membrane to various concentrations of CO_2 and subsequent exposure to background air at 40% RH and at 25 °C. ◆ With Membrane X Without Membrane.

that the thermal stability of PABA is greater than that of other self-doped forms of polyaniline. When exposed to above 400 °C, polyaniline experiences complete decomposition of the backbone, while PABA remains intact and possesses a high level of conductivity. The increase in resistance value with exposure to −25 °C may be explained by the change in the morphology of the film and the restriction of the transportation of charge carriers.

The percentage sensitivity as a response to temperature is defined as:

$$S = \left[\frac{T2 - T1}{T1}\right] 100 \quad (7)$$

where T2 is the resistivity of the PABA sensor for temperature level 2, and T1 is the resistivity of the PABA sensor for temperature at level 1.

PABA–Nafion sensor's sensitivity shows saturated response to analyte between 25 °C and 45 °C (Fig. 8). The sensitivity of the sensor decreases above 45 °C. The conductivity of PABA decreases with loss of moisture from the sensing material. Thermal curing influences the chain alignment of the polymer leading to increased conjugation length and charge transfer between the polymer chains and dopants, leading to increased conductivity (Kulkarni, Viswanath, & Khanna, (2005); Li, Josowics, Janata, and Semancik (2004)). Heating might cause molecular rearrangement on the material which might make the molecular conformation favourable for electron delocalisation (Kulkarni, Viswanath, Marimuthu, & Seth, 2004). There may be changes in the morphology of the thin film which might restrict the transportation of charge carriers over the polymer chains resulting in the decreased resistivity.

The sensor did not respond to various CO_2 concentrations and the response became noisy above 55 °C. To assess the influence of temperature, experiments were conducted at 50% RH for measurements at 25 °C. As the temperature increased from 25 to 55 °C, the water molecules in the air might have been reduced. Further investigations are needed to evaluate the performance of PABA–Nafion sensor at various temperatures and at higher humidity levels.

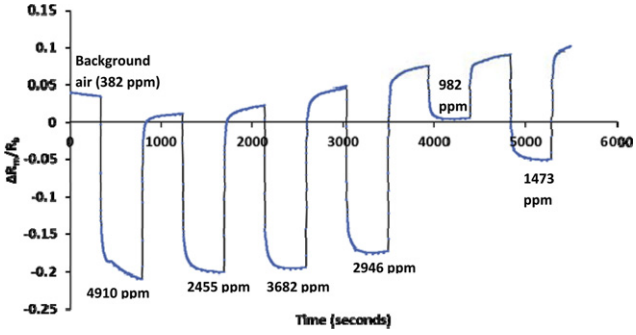

Fig. 12 – Response of the PABA–Nafion sensor operated in random mode to various concentrations of CO_2 and subsequent exposure to background air at 40% RH and at 25 °C.

3.4. *Repeatability and reproducibility*

Sensor repeatability refers to the successive runs made using a single sensor to evaluate discrepancies in its response. Sensor reproducibility refers to the sensor variations in response between individual chips of a batch of similarly

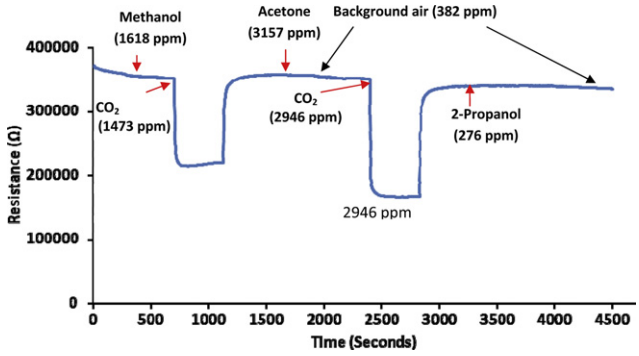

Fig. 14 – Response of the PABA sensor with selective gas permeable PTFE membrane to CO_2, methanol, acetone and 2-propanol analytes at 40% RH and at 25 °C. ← Injection point of the analytes.

constructed sensors. The repeatability of the sensor was studied by using the same sensor to repeatedly (five times) measure the response to different CO_2 concentrations (Fig. 9). At the same time, the reproducibility of the sensor was studied by using five similarly constructed sensors to measure the response at various CO_2 gas levels (Fig. 10).

In the reproducibility study, the same response trend was observed for all of the sensors on the same chip. Each sensor chip has seven sensors and the response of the sensors is shown in Fig. 9. The response of the sensors was not stabilised initially and over the course of time, it became stabilised. The relative standard deviation (R.S.D.) for reproducibility of the sensor was 11%. Variation in the response of the sensor could be due to the construction variation and operational variation. The sensitivity got better with time/exposure as trial 4 and trial 5 responses are nearly overlapping. The same trend was observed for all sensor electrodes in different chips (data not shown).

3.5. *Dynamic characteristics*

Sensitivity, linearity, accuracy, drift and hysteresis properties have transient effects that are settled to their steady state and are the static characteristics of a sensor. The experimental results on the effect of humidity and temperature indicate that the response of the PABA–Nafion sensor to various levels of CO_2 is linear up to 2455 ppm and above that a saturation effect is observed. Prior to actual measurements, the sensor was exposed for 20 min in the background gas flow to achieve stabilised response and to reduce associated drift. The repeatability and reproducibility experiments results show that the PABA–Nafion sensor behaves with higher sensitivity. A sensor's sensitivity indicates how much the sensor's output changes upon exposure to analyte. Drying the sensor electrodes after material deposition over 30 min reduced the drift to a large extent.

The dynamic characteristics of a sensor are determined by analysing the response of the sensor to variable input of analyte (CO_2) concentrations such as step mode, ramp mode (Fig. 11) and random measurement (Fig. 12). Characterisation of the PABA–Nafion sensor's dynamic response was evaluated by comparing the step mode and ramp mode measurement. The ramp mode response curve shows that the PABA–Nafion sensors did not respond to CO_2 levels above 2455 ppm. The step or pulsed mode measurement shows that the response curve was reversible upon exposure to background gas.

3.6. *Evaluation of gas permeable membrane*

The gas permeable membranes play an important role in limiting the diffusion rate of CO_2 as well as selectively passing the analyte into the electrolyte reservoir. By selecting appropriate gas permeable membranes with different pore size and thickness, the sensitivity and (or) the linear range of the sensor can be optimised to a certain extent. The membranes act as a protecting cover for the electrolyte and the sensing material in the sensing reservoir on the electrode arrays. The PTFE membrane is highly selective to CO_2 and does not allow other gas molecules to pass through hence aiding in reducing the cross-sensitivity effect of the sensor (Fig. 13).

3.7. *Effect of cross sensitivity*

For efficient functioning of sensors, there is a need to find out whether the sensor is interfered with by other gases in addition to the target analyte gas. The dc resistance values decreased with increasing CO_2 concentration indicating an increase of conductivity due to CO_2 concentration levels. But upon random exposure of 1% (percent of vapour pressure) of methanol (1618 ppm), acetone (3157 ppm) and 1-propanol (276 ppm) (representative of compounds expected in stored grain (Borjesson, Stollman, Adamek, & Kaspersson, 1989; Loschiavo et al., 1986)) in air for 3 min, followed by various levels of CO_2 did not change the resistivity of the sensor. The PABA–Nafion sensor works on the principle of pH change and CO_2 being acidic reacts with the electrolyte to induce ionic exchange resulting in decreased resistivity. The gas permeable membrane is selective to CO_2 and allows only CO_2 molecules to pass through. Hence there was no response (Fig. 14) to alcohols or ketones in air.

3.8. *Sensor packaging*

Miniature sensor elements will usually not function on their own. The sensor packaging gives the sensor a suitable shape or form, provides electrical connection to the sensor, and provides a window from the sensor to the outside world. In addition, the sensor elements need mechanical and chemical protection. To package the CO_2 sensor for preliminary testing in bulk grain, several options were considered to ensure that the packaging components avoid contamination of the sensing material and the substrate by undesirable materials including grain dust and foreign material in grain. The dimensional details of the sensor chip and gas diffusion

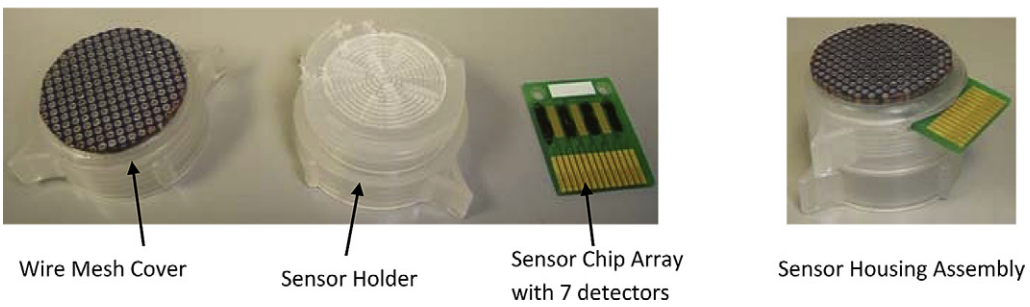

Fig. 15 – Picture of the Sensor Housing Assembly Packaging.

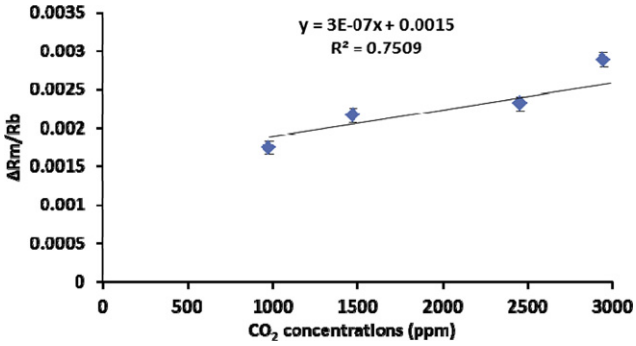

Fig. 16 – Response of PABA Nafion Sensor with packaging kept inside grain bulk to concentrations of CO_2 at 50% RH and at 25 °C.

properties of the packaging material were considered in selecting the packaging components. The performance characteristics of the sensors depend on the geometry of electrodes, thermal design of the structure and the nature of the electronic interface. On practical applications, there will be a tradeoff between cost and performance.

3.9. *Sensor's performance inside simulated grain bulk*

The CO_2 sensor packaged in the prototype housing assembly (Fig. 15) was tested in plastic pails (4 l capacity) filled with wheat. The pails were purged with known CO_2 concentrations to simulate spoilage of grain. The sensor exhibited excellent response (Fig. 16) to change in CO_2 levels inside grain bulk. The CO_2 gas at desired levels was passed through the bottom of the pail while the sensor was kept immersed in the grain bulk at the top. The plastic pail was covered tightly with duct tape to prevent atmospheric exchange into the grain bulk. Gas samples from the outlet tube were analysed using GC–MS to determine the concentrations of the outlet gas.

4. Conclusions

A sensitive tool for detecting incipient or ongoing deterioration of stored grains by measuring CO_2 levels was developed using PABA conducting polymer. The CO_2 sensor can monitor the CO_2 concentration, which requires water in the air to operate, permitting the detection of CO_2 between 20 and 70% equilibrium relative humidity. The sensor dynamically detected up to 2455 ppm of CO_2 levels in the grain bulk. The CO_2 sensor exhibited dynamic performance in its response, recovery time, sensitivity, selectivity, stability and response slope. The CO_2 sensor responded well to various concentrations of CO_2 at temperatures between 25 °C and 55 °C. The sensors respond to various levels of CO_2 at ambient temperature without artificial cooling. The packaging unit allowed measurement of CO_2 concentration in grain bulk. The methodology used for building the CO_2 sensor device is compatible with the MEMS process (printed circuit board process) and can be mass manufactured using screen printing technology.

Acknowledgements

We thank the Natural Sciences and Engineering Research Council of Canada and the Canada Research Chairs program for their financial support for this project.

REFERENCES

Borjesson, T., Stollman, U., Adamek, P., & Kaspersson, A. (1989). Analysis of volatile compounds for detection of molds in stored cereals. *Cereal Chemistry, 66*(4), 300–305.

Breck, D. W. (1974). *Zeolite molecular Sieves*. New York: John Wiley & Sons Inc.

Deore, B. A., Braun, M. D., & Freund, M. S. (2006). pH dependent equilibria of poly(anilineboronic acid)-saccharide complexation in thin films. *Macromolecular Chemistry and Physics, 207*, 660–664.

Deore, B. A., & Freund, M. S. (2009). Self doped polyaniline nanoparticle dispersions based on boronic acid-phosphate complexation. *Macromolecules, 42*, 164–168.

Dickinson, T. A., White, J., Kauer, J. S., & Walt, D. R. (1998). Current trends in artificial nose technology. *Trends in Biotechnology, 16*(6), 250–258.

English, J. T., Deore, D. A., & Freund, M. S. (2006). Biogenic amine vapor detection using poly(anilineboronic acid) films. *Sensors and Actuators B, 115*, 666–671.

FAO. (2000). *Crop and food supply assessment. FAO corporate document depository: Economic and social department*. Rome, Italy: United Nations.

Fabre, B., & Taillebois, L. (2003). Poly(aniline boronic acid)-based conductimetric sensor of dopamine. *Chemical Communications, 24*, 2982–2983.

Fuke, M. V., Vijayan, A., Kanitkar, P., Kulkarni, M., Kale, B. B., & Aiyer, R. C. (2008). Ag-polyaniline nanocomposite cladded planar optical waveguide based humidity sensor. *Journal of Materials Science: Materials in Electronics, 20*(8), 695–703.

Hu, I., Vincenzo, B., Vincenzo, T., Antonino, A., & Vincenzo, A. (2008). PEO-PPO-PEO triblock copolymer/Nafion blend as membrane material for intermediate temperature. *DMFCs Journal of Applied Electrochemistry, 38*(4), 543–550.

Ileleji, K. E., Maier, D. E., Bhat, C., & Woloshuk, C. P. (2006). Detection of a developing hot spot in stored corn with a CO_2 sensor. *Applied Engineering in Agriculture, 22*, 275–289.

Jensen, M. A., & Rechnitz, G. A. (1979). Response time characteristics of the pCO2 electrode. *Analytical Chemistry, 51*(12), 1972–1977.

Jurs, P. C., Bakker, G. A., & McClelland, H. E. (2000). Computational methods for the analysis of chemical sensor array data from volatile analytes. *Chemical Reviews, 100*(7), 2649–2678.

Kulkarni, M. V., Viswanath, A. K., & Khanna, P. K. (2005). Synthesis and humidity sensing properties of conducting poly (N-methyl aniline) doped with different acids. *Sensors and Actuators B, 115*, 140–149.

Kulkarni, M. V., Viswanath, A. K., Marimuthu, R., & Seth, T. (2004). Synthesis and characterization of polyaniline doped with organic acids. *Journal of Polymer Science Part A: Polymer Chemistry, 42*(8), 2043–2049.

Li, G., Josowics, M., Janata, J., & Semancik, S. (2004). Effect of thermal excitation on intermolecular charge transfer efficiency in conducting polyaniline. *Applied Physics Letters, 85*(7), 1187–1189.

Loschiavo, S. R., Wong, J., White, N. D. G., Pierce, H. D., Borden, J. H., & Oehlschlager, A. C. (1986). Field evaluation of a pheromone to detect adult rusty grain beetles, cryptolestes ferrugineus

(coleoptera: cucujidae), in stored grain. *The Canadian Entomologist, 118*, 1–8.
Muir, W. E., Waterer, D., & Sinha, R. N. (1985). Carbon dioxide as an early indicator of stored cereal and oilseed spoilage. *Transactions of the ASAE, 28*, 1673–1675.
Neethirajan, S., Jayas, D. S., & Sadistap, S. (2009). Carbon dioxide (CO2) sensors for the agri-food industry – a review. *Food and Bioprocess Technology, 2*, 115–121.
Ostwal, M. M., Pellegrino, J., Norris, I., Tsotsis, T. T., Sahimi, M., & Mattes, B. R. (2005). Water sorption of acid-doped polyaniline solid fibers: equilibrium and kinetic response. *Industrial & Engineering Chemistry Research, 44*(20), 7860–7867.
Parvatikar, N., Jain, S., Kanamadi, C. M., Chougule, B. K., Bhoraskar, S. V., & Prasad, M. V. N. A. (2006). Humidity sensing and electrical properties of polyaniline/cobalt oxide composites. *Journal of Applied Polymer Science, 103*(2), 653–658.
Parvatikar, N. S., Jain, S., Khasim, M., Revansiddappa, S. V., Bhoraskar, M. V. N. A., & Prasad, S. (2006). Electrical and humidity sensing properties of polyaniline/WO3 composites. *Sensors and Actuators B, 114*, 599–603.
Prokes, J., & Stejskal, J. (2004). Polyaniline prepared in the presence of various acids 2. Thermal stability of conductivity. *Polymer Degradation and Stability, 86*, 187–195.
Schaller, E., Bosset, J. O., & Escher, F. (1998). Electronic noses and their application to food. *Lebensmittel-Wissenschaft und-Technologie, 31*(4), 305–316.
Semple, R. L., Hicks, P. A., Lozare, V., & Castermans, A. (1988). Towards integrated commodity and pest management in grain storage. In *Proceedings of the Integrated Pest management Strategies in grain storage systems Conference*. Philippines: National Post Harvest Institute for Research and Extension (NAPHIRE), Department of Agriculture. June 6–18.
Shoji, E., & Freund, M. S. (2002). Potentiometric saccharide detection based on the pKa changes of poly(aniline boronic acid). *Journal of American Chemical Society, 124*, 12486–12493.
Singh (Jayas), D., Muir, W. E., & Sinha, R. N. (1983). Finite element modelling of carbon dioxide diffusion in stored wheat. *Canadian Agricultural Engineering, 25*, 149–152.
Skotheim, T. A., Elsenbaumer, R. L., & Reynolds, J. R. (1998). *Handbook of conducting polymers*. Boca Raton, FL: CRC Press.
Suri, K., Annapoorni, S., Sarkar, A. K., & Tandon, R. P. (2002). Gas and humidity sensors based on iron oxide-polypyrrole nanocomposites. *Sensors and Actuators B, 81*, 277–282.
USDA. (2007). *Foreign Agricultural Service Report. World Agricultural production circular Series Wap 04–07*. Baltimore, MD: United States Department of Agriculture.
Virji, S., Huang, J., Kaner, R. B., & Weiller, B. H. (2004). Polyaniline nanofiber gas sensors: examination of response mechanisms. *Nanoletters, 4*, 491–496.
Viswanathan, B., & Helen, M. (2007). Is Nafion the only choice? *Bulletin of the Catalysis Society of India, 6*, 50–66.
Wallace, H. A. H., & Sinha, R. N. (1981). Causal factors operative in distributional patterns and abundance of fungi: a multivariate study. In *The Fungal Community– its Organisation and role in Ecosystems* (pp. 233–247). New York, NY: Marcel Dekker Inc.
Yu, I., Deore, B. A., Recksiedler, C. L., Corkery, C., Abd-El-Aziz, A. S., & Freund, M. S. (2005). Thermal stability of high molecular weight self-doped poly(aniline boronic acid). *Macromolecules, 38*, 10022–10026.